Supplement of Biogeosciences, 23, 3073–3090, 2026
https://doi.org/10.5194/bg-23-3073-2026-supplement

Biogeosciences Open Access EGU

Supplement of

Unexpected quasi-independence of coloured dissolved organic matter absorption from chlorophyll-*a* concentration in the Southern Ocean

Juan Li et al.

Correspondence to: Juan Li (juan.li@takuvik.ulaval.ca)

Table S1 Number (N) of BGC-Argo float profiles eliminated based on various criteria and quality controls used in this study. Criteria are successively applied as they appear in this Table, which is why the number of "Bad chlorophyll profile" and "Bad b_b(700 nm) profile" can be different for each spectral band.

	Southern Ocean < 40° S			Low-latitude Ocean 40° S to 60° N		
N floats	60			211		
N profiles, total	10,579			35,591		
N discarded profiles						
Depth < 200 m	30			1,396		
Sun elevation < 15°	2,472			4,997		
	380 nm	412 nm	490 nm	380 nm	412 nm	490 nm
Out-of-range Z_{pd}	2,516	2,600	2,563	12,294	12,708	12,281
$K_d < K_w$	14	45	279	379	961	2,649
Bad chlorophyll profile‡	0	0	0	25	23	23
Bad b_b(700 nm) profile‡	488	482	469	1,741	1,652	1,584
Bad E_d profile‡, per band	2	2	2	4	4	3
Surface average $b_{bp} < 0$	28	27	29	764	681	617
Retrieved a_y values < 0	76	191	996	374	859	3,582
Number of profiles used	4,953	4,730	3,739	13,617	12,310	8,459

‡ from any flag other than "A" or "B" following the BGC-Argo nomenclature (Argo data management, 2025). Synthetic BGC Argo netCDF files have been used (file extension "Sprof").

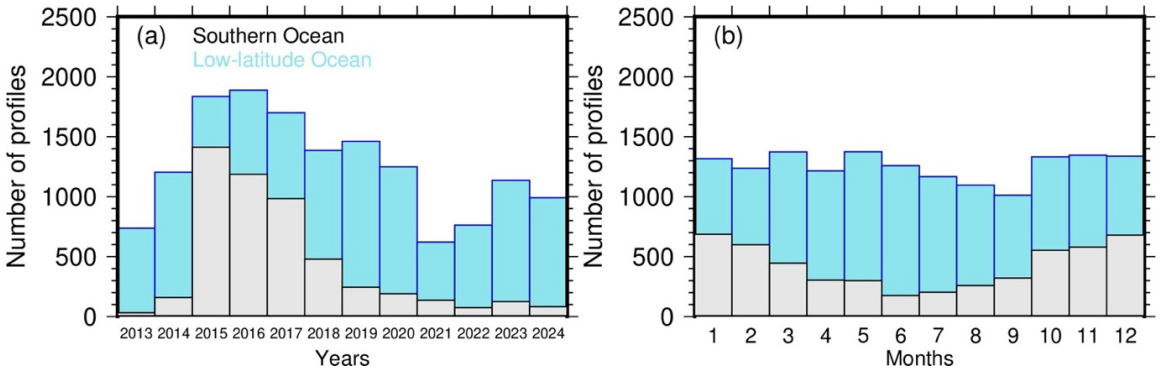

Figure S1: Time distribution of the selected set of BGC-Argo profiles over (a) years and (b) months.

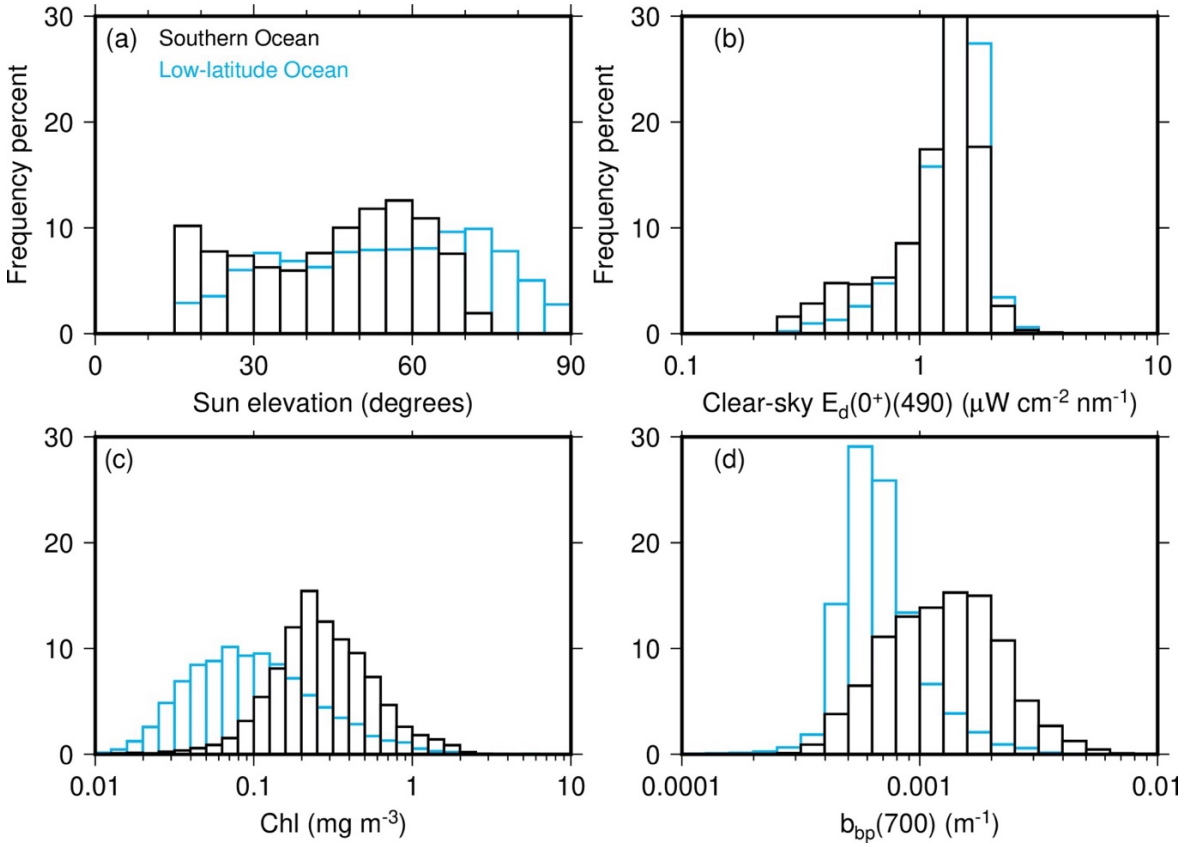

Figure S2: Distribution of (a) sun elevation, (b) measured downward irradiance at 490 nm for values within 20% of the clear-sky value calculated following Gregg and Carder (1990) (data outside of this range are also used, however), (c) Chl and (d) b_{bp} at 700 nm.

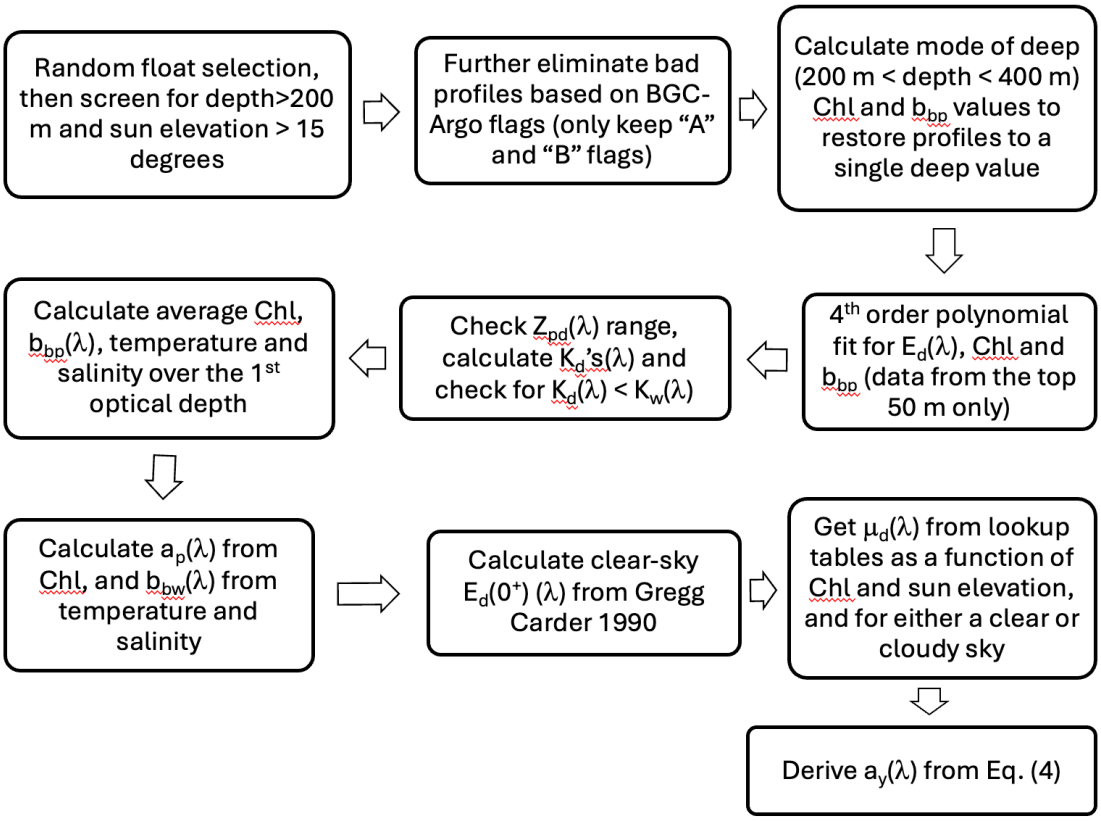

Figure S3: Workflow for the processing of the BGC-Argo data, from profiles of $E_d(\lambda)$, b_{bp} at 700 nm and Chl, down to deriving the CDOM absorption coefficient a_y.

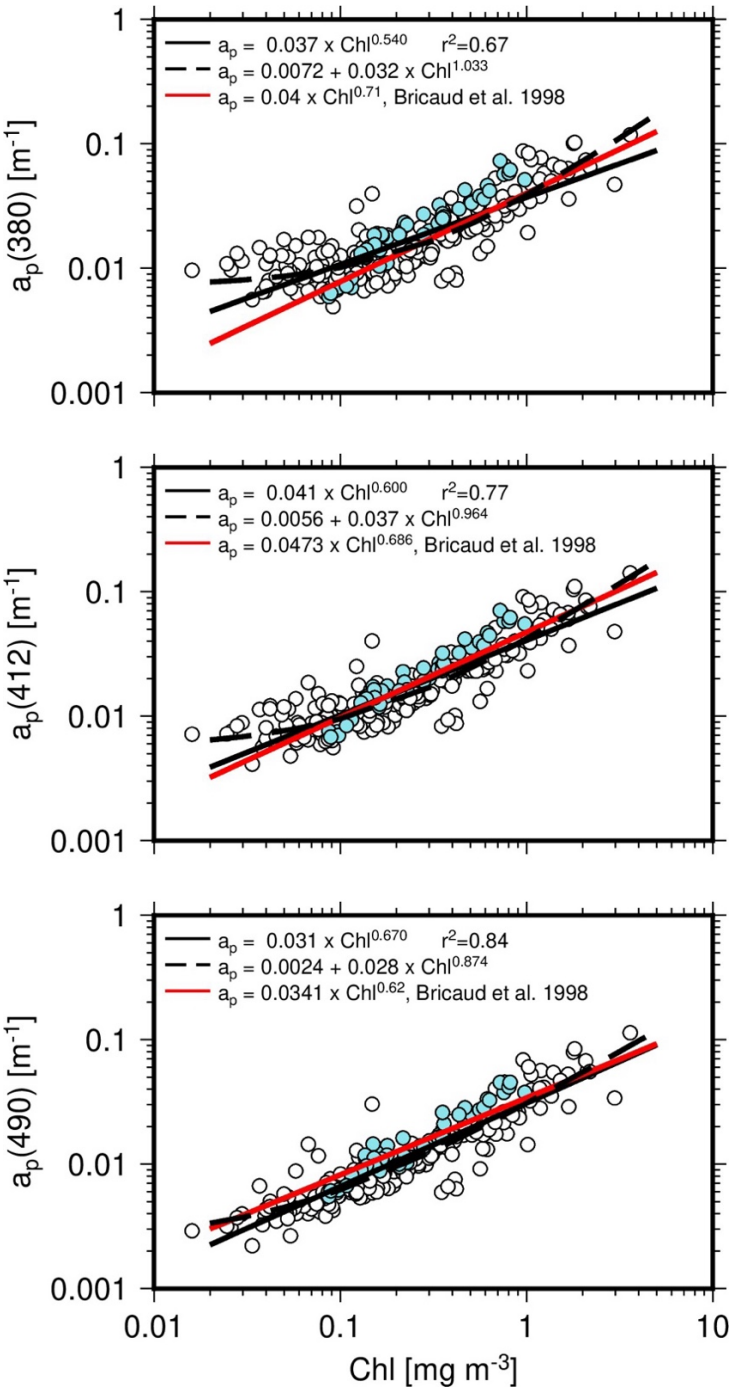

Figure S4: Particulate absorption coefficient at the three wavelengths indicated as a function of Chl. The data are from the ACE (open dots) and SOLACE (turquoise) research voyages. The solid black lines are linear fits on the log-transformed data. The dashed black lines are non-linear fits (Eq. 5) on the same data. The red lines are the parameterization from Bricaud et al., (1998).

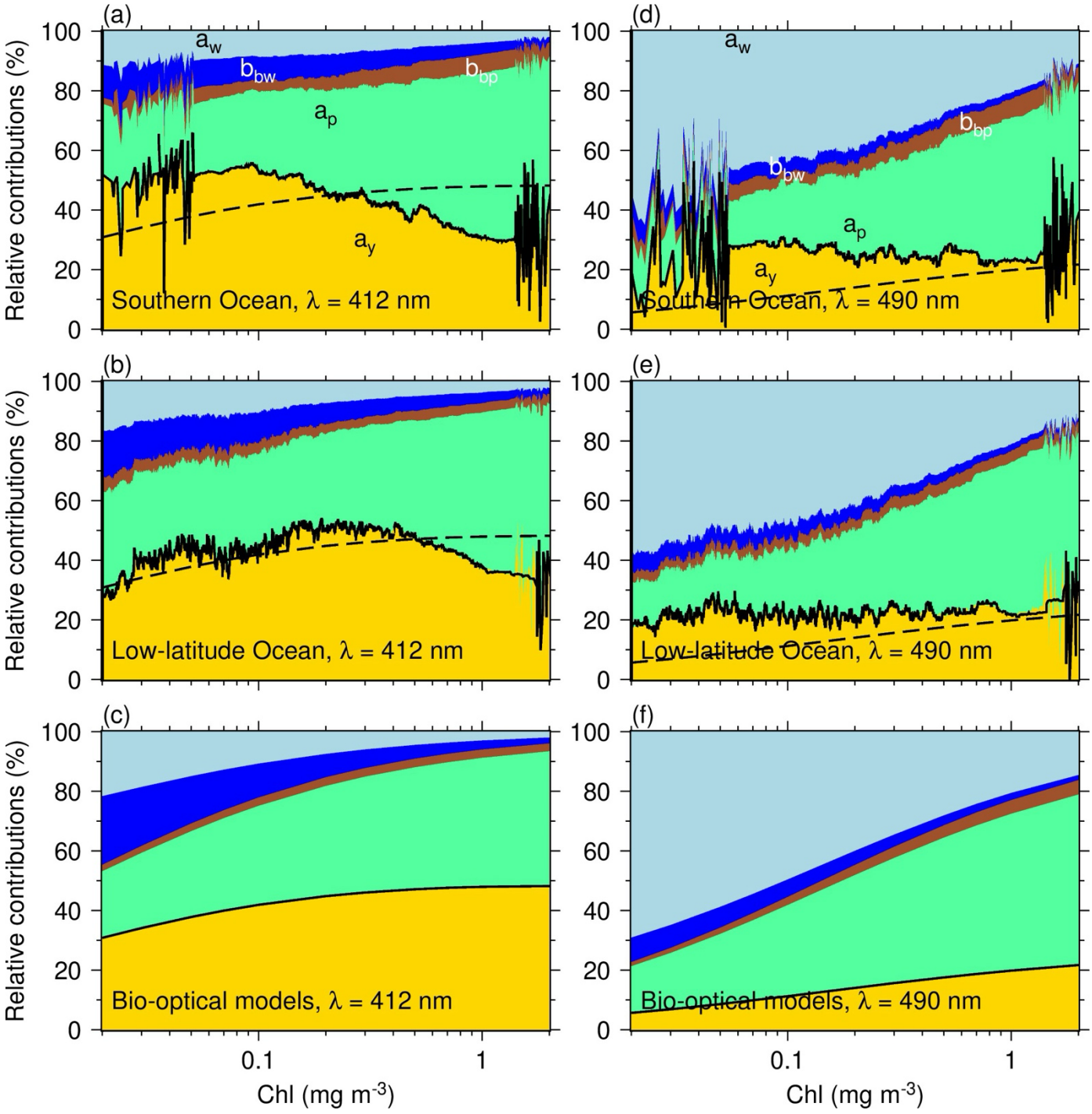

Figure S5: Relative contributions of a_w (light blue), b_{bw} (blue), b_{bp} (brown), a_p (green) and a_y (gold) in Eq. (4) at λ = 412 and 490 nm, as a function of Chl. Panels (a,d) are for the SO, (b,e) for the low-latitude Oceans, and (c,f) are when using Bricaud et al., (1998) to calculate a_p, MG09 for a_y, and MM01 for b_{bp}. The thick black line delineates the contribution of a_y to the budget. This modelled relative contribution of a_y from panel (c,f) is reproduced in other panels as a dashed line. The increased noise in the curve for Chl < 0.03 mg m^{-3} and Chl > ~1.5 mg m^{-3} arises from the low numbers of retrievals in these ranges.